1992

Pressure Distributions Along Eccentric Circular Valve Reeds of Hermetic Compressors

J. L. Gasche
Federal University of Santa Catarina; Brazil

R. T. S. Ferreira
Federal University of Santa Catarina; Brazil

A. T. Prata
Federal University of Santa Catarina; Brazil

PRESSURE DISTRIBUTIONS ALONG ECCENTRIC CIRCULAR VALVE REEDS OF HERMETIC COMPRESSORS

J.L. Gasche, R.T.S. Ferreira, A.T. Prata

Department of Mechanical Engineering
Federal University of Santa Catarina
Florianopolis, SC - 88049 - Brazil

ABSTRACT

An experimentally validated analysis of the incompressible, laminar and isothermal flow in eccentric radial diffusers, representing a laboratory model of compressors valve system is numerically performed. The experimental procedures and the experimental setup are concisely described. Pressure distributions along the three-dimensional flow and the resultant axial force acting on the frontal disk are presented for various flow Reynolds numbers, different axial gaps and eccentricities. A three-dimensional bicylindrical coordinate system is used to obtain a description of the whole flow field. Certain characteristics of the velocity field are also presented.

NOMENCLATURE

D - frontal disk diameter, m
d - feeding orifice diameter, m
s - axial gap between disks, m
l - feeding orifice length, m
e - eccentricity between feeding orifice and frontal disk center lines, m
p - pressure, Pa
u, v, w - velocity components in ψ, η and z directions, m/s
ψ, η, z - bicylindrical coordinates
h - square root of the metric of the bicylindrical coordinate system, m
$\bar{p}$ - dimensionless pressure
$\bar{v}$ - mean velocity through the feeding orifice, m/s
Re - Reynolds number, $Re = \rho \bar{v} d/\mu$
F - dimensionless force on the frontal disk
Vm - mean velocity in a determined diffuser cross section, m/s
ρ - fluid density, kg/m^3
μ - absolute viscosity, kg/ms

INTRODUCTION

The operating cycle of a high speed positive displacement compressor can be described by a series of complex phenomena which show high degree of interaction and happen in a short period of time. The mathematical model used in a compressor simulation program requires the equations describing the reed dynamic behavior. Therefore it is necessary to fully understand the flow field of the gas flowing through the valve system, especially when automatic valves are employed, that is, the flow field is responsible for opening and closing those reed type valves.

Deschamps [01] and Ferreira et al. [02] have performed an experimentally validated numerical analysis of the laminar, incompressible and isothermal air flow through concentric radial diffusers with the purpose of understanding the flow through compressor valves. Deschamps [01] presents a very broad bibliographic survey related to the subject. However, as very few compressor valves systems show this type of concentricity. In order to improve the

model, getting it closer to actual refrigerating compressors valve systems, the analysis of the flow through eccentric radial diffuser, as shown in Fig. 1, is performed in this work.

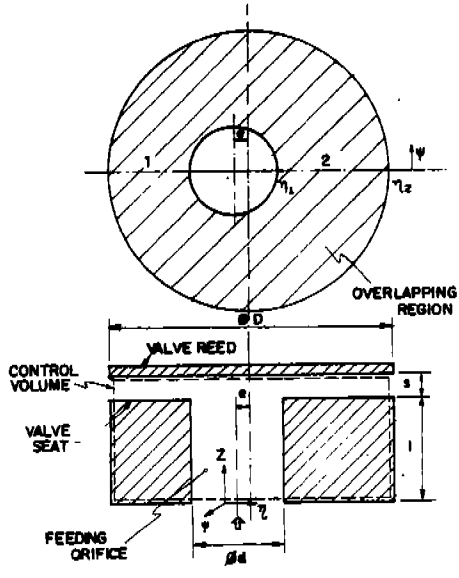

Fig. 1 - Flow geometry

It can be observed from Fig. 1 that the presence of eccentricity between the feeding orifice and the frontal disk, which is similar to a reed with parallel displacement, generates circular regions with different overlappings. This situation causes a non-uniform circumferential distribution of mass flow rate leaving the feeding orifice. The flow adjusts itself according to the solid boundaries in such a way that the main velocity component in the diffuser region, v, increases progressively from region(2) to (1). This fact produces an asymmetric pressure distribution on the frontal disk and therefore the flow is three-dimensional.

The main objective of this work is to present the numerical results of the laminar, incompressible, isothermal, steady air flow through eccentric radial diffusers. The numerical model has been validated by means of the good agreement reached with experimental pressure distributions on the frontal disk. Numerical results for the pressure distribution and the total force on the reed and also some details of the velocity field are presented. The experimental procedures and the experimental test rig are concisely described.

PROBLEM FORMULATION

The geometry of the eccentric diffuser under analysis has to be described by a bicylindrical coordinate system (ψ,η,z), as shown in Fig. 1. The air flows axially (direction z) through the feeding orifice with diameter d and length l and, after being deflected by the frontal disk of diameter D, it is forced through the gap s between disks in directions ψ and η. The disk with the feeding orifice is analogous to the valve seat and the frontal disk corresponds to the valve reed.

The hydrodynamic flow problem is governed by the continuity and Navier-Stokes equations, (1)-(4), written in bicylindrical coordinates for laminar, incompressible, isothermal and steady conditions.

$$1/h^2[\partial(\rho hu)/\partial\psi + \partial(\rho hv)/\partial\eta + \partial(\rho h^2 w)/\partial z] = 0 \qquad (1)$$

$$1/h^2[\partial(\rho huu)/\partial\psi + \partial(\rho hvu)/\partial\eta + \partial(\rho h^2 wu)/\partial z] =$$

$$-1/h\ \partial p/\partial\psi + \mu/h^2[\partial^2 u/\partial\psi^2 + \partial^2 u/\partial\eta^2 + h^2\partial^2 u/\partial z^2] +$$

$$+ \mu/h^2[2/h.\partial h/\partial\eta.\partial v/\partial\psi - 2/h.\partial h/\partial\psi.\partial v/\partial\eta -$$

$$- u/h(\partial^2 h/\partial\psi^2 + \partial^2 h/\partial\eta^2)] - \rho/h^2[uv.\partial h/\partial\eta - v^2.\partial h/\partial\psi] \qquad (2)$$

$$1/h^2[\partial(\rho huv)/\partial\psi + \partial(\rho hvv)/\partial\eta + \partial(\rho h^2 wv)/\partial z] =$$

$$- 1/h\ \partial p/\partial\eta + \mu/h^2[\partial^2 v/\partial\psi^2 + \partial^2 v/\partial\eta^2 + h^2\partial^2 v/\partial z^2] +$$

$$+ \mu/h^2[2/h\ .\ \partial h/\partial\psi\ .\ \partial u/\partial\eta - 2/h\ .\ \partial h/\partial\eta\ .\ \partial u/\partial\psi\ -$$

$$- v/h\ .\ (\partial^2 h/\partial\eta^2 + \partial^2 h/\partial\psi^2)] - \rho/h^2[uv\ .\ \partial h/\partial\psi - u^2.\partial h/\partial\eta] \qquad (3)$$

$$1/h^2\ [\partial(\rho huw)/\partial\psi + \partial(\rho hvw)/\partial\eta + \partial(\rho h^2 ww)/\partial z] =$$

$$- \partial p/\partial z + \mu/h^2[\partial^2 w/\partial\psi^2 + \partial^2 w/\partial\eta^2 + h^2\ \partial^2 w/\partial z^2] \qquad (4)$$

where u, v and w are the velocity components in the ψ, η and z directions, respectively, p is the pressure, ρ is the fluid density, μ is the absolute viscosity and h is the square root of the metric related to the bicylindrical coordinate system.

It is easily shown that h is given by

$$h = a/(\cosh\eta - \cos\psi) \qquad (5)$$

where a is the geometric parameter of the coordinate system.

The boundary conditions needed for the whole specification of the problem are given by Eqs. (6).

$$u = v = w = 0 \quad \text{for} \quad z = 1 + s;\ \eta = \eta_2\ ;\ 0 \le \psi \le 2\pi \qquad (6a)$$

$$u = v = w = 0 \quad \text{for} \quad 0 \le z \le 1;\ \eta = \eta_2\ ;\ 0 \le \psi \le 2\pi \qquad (6b)$$

$$u = v = 0 \quad \text{for} \quad z = 0\ ;\ \eta \ge \eta_1\ ;\ 0 \le \psi \le 2\pi \qquad (6c)$$

$$u = v = w = 0 \quad \text{for} \quad z = 0\ ;\ \eta_2 \le \eta \le \eta_1\ ;\ 0 \le \psi \le 2\pi \qquad (6d)$$

$$w = \partial(\rho hu)/\partial\eta = \partial(\rho hv)/\partial\eta = 0 \quad \text{for} \quad 1 \le z \le 1 + s;\ \eta = \eta_2\ ;$$

$$0 \le \psi \le 2\pi \qquad (6e)$$

NUMERICAL SOLUTION

The differential equations (1)-(4) governing the laminar flow field and the associated boundary conditions (6) are discretized using the finite volume methodology developed by Patankar [03]. The detailed discretization of all the equations is presented by Gasche [04].

The solid region of the valve seat, belonging to the calculation domain has been treated as a fluid with infinite viscosity, according to Patankar [05].

For the special case of the eccentric radial diffuser, the numerical model has to consider a zero gauge reference pressure at the diffuser outlet, that is, $p = 0$ for $1 \leq z \leq 1 + s$; $\eta = \eta_2$ and $0 \leq \psi \leq 2\pi$. In order to reach this boundary condition the control volumes at the exit of the diffuser are made sufficiently small and the main coefficient for the correction of the pressure equation, related to the SIMPLE algorithm, are made very big. Smaller control volumes, in the η direction, will guarantee a better approximation for the zero reference pressure at the diffuser outlet.

Due to the presence of very high pressure and velocity gradients, special attention has been devoted to the mesh selection in order to minimize the contribution of false diffusion. The final mesh used to generate the results in this work has 30240 nodal points, being 14 points in ψ-direction, 54 points in η-direction and 40 points in z - direction.

EXPERIMENTAL SETUP AND PROCEDURES

Fig. 2 presents a schematic general view of the experimental setup. Compressed air stored in three tanks of 0.450 m^3 each one and maximum pressure of 12 bar flowed through a 75mm diameter and 6.5m long PVC horizontal straight pipe before reaching the test section. A flow rate control valve and a calibrated orifice flow meter are mounted in the pipeline. The test section is composed by the valve seat, an aluminum disk (ϕ 150 mm, l = 28 mm) containing the feeding orifice (ϕ 30 mm), by the valve reed, a stainless steel disk (ϕ 90 mm) with a sliding bar and a small tap hole in order to measure the pressure distribution, and the positioning system used to furnish the desired location for the valve reed. The valve reed, represented in the experiment by the frontal disk, has a special feature as shown in Fig. 3. Along the horizontal reed diameter there is a sliding bar provided with a small tap hole (ϕ 0.7 mm) and an internal connecting perforation up to one of the ends of the bar and then connected to a differential pressure inductive transducer. At the other end of the sliding bar an inductive displacement transducer is attached in order to supply the instantaneous horizontal position of the tap hole. Both signals from the inductive transducers are introduced in an amplifier bridge and after to a microcomputer provided with an AD converter. All the analogic signals are adequately treated by a data acquisition program which is able to register pressure signals in intervals of 0.5mm.

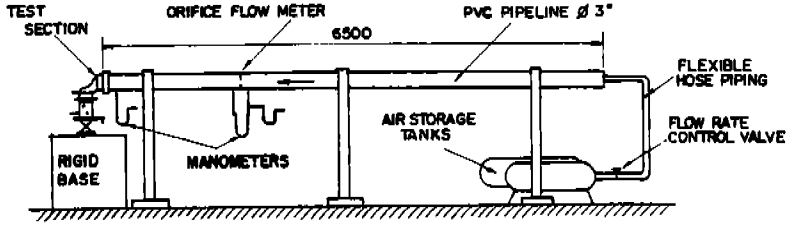

Fig. 2 - Schematic view of the experimental setup

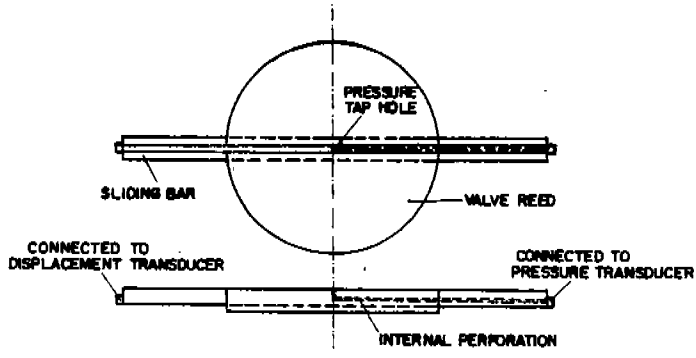

Fig. 3 - Valve reed with sliding tap hole

The reed positioning system, shown in Fig. 4, is composed by 5 moving tables. Initially, both disks have to be concentric, parallel and placed at a certain distance one from the other. Additional information regarding the experimental setup are available in [04].

Before starting to take data, some adjustments are carried out in the experimental setup. First of all the reference zero separation of the disks is determined. The frontal disk is carefully positioned using a mask drawn in the valve seat assuring the concentricity and the alignment of both disks. One steel sphere with diameter of 3.174mm glued to a fine thread is slid in different positions between the disks in order to verify their parallel displacement. Fine adjustments in the angular table produces a uniform sliding for the sphere everywhere in the gap. The final verification is made using the proper pressure distribution along the frontal disk. For the highest desired flow rate, at a certain separation between disks, the symmetry of the pressure profile is then checked. If this symmetry is not achieved within 2%, the whole procedure is repeated as many times as necessary. The accuracy in positioning the frontal disk is less than 0.01 mm.

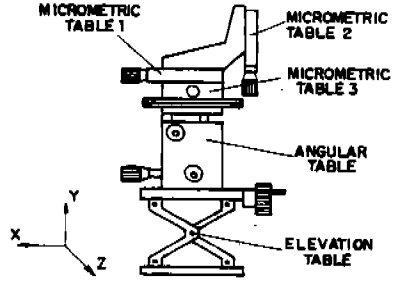

Fig. 4 - Valve positioning system

A very important aspect that has to be considered is the modification in the disks gap due to the forces produced by the pressure distribution especially for small gaps and high Reynolds numbers. Two inductive displacement transducers measured the differential displacement in both disks during the tests. Those values are used to correct the data. Table 1 shows the corrections in the

disks separation due to pressure distribution.

The main quantities measured during the experiment are: horizontal pressure distribution on the reed, mass flow rate, gap between reed and seat and eccentricity between reed and feeding orifice. The pressure distribution is measured with an inductive pressure transducer with a full scale of 0.01 bar or 0.1 bar for higher pressures.

The uncertainty associated to the experimental results reaches values on the order of 1% for the dimensionless pressure distribution on the reed, according to Holman [06]. However, if one takes into account the contribution of the uncertainty in the disks gap, due to the great influence of this distance s, the uncertainty for the dimensionless pressure distribution is less than 10%, as reported in [04].

Table 1 - Corrections introduced in disks gap for s/d = 0.01.

Re	Correction [μm]
3000	30
2500	25
2000	23
1500	18
1000	12
500	9

RESULTS

Two typical comparisons between experimental and numerical results for the pressure distribution on the reed are presented in Figs. 5 and 6. In the ordinate axis it is represented the local dimensionless pressure given by $p/(1/2\ \rho\ \bar{u}^2)$, where $\bar{u}$ is the mean velocity in the feeding orifice. In the abscissa it is plotted the dimensionless radial position r/d. The flow Reynolds number is defined as $Re = \rho \bar{u} d/\mu$. The validation of the numerical model is evident from the good comparison between experimental and numerical results.

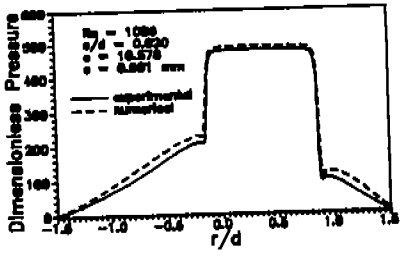

Fig. 5 - Comparison of numerical and experimental results for Re=1086, s/d=0.02 and e=10.578mm

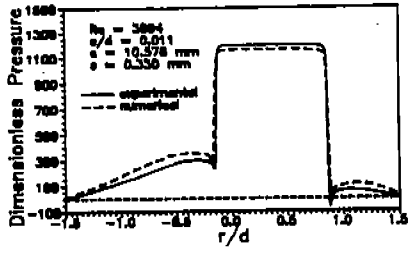

Fig. 6 - Comparison of numerical and experimental results for Re=3094, s/d=0.011 and e=10.578mm

The numerical results for the horizontal pressure distributions on the reed are presented in Figs. 7 to 12, for three different Reynolds numbers of 500, 1500 and 3000, each one for two different dimensionless gaps between disks of 0.01 and 0.03 and each one for four horizontal eccentricity values of 0, 5, 10 and 15 mm.

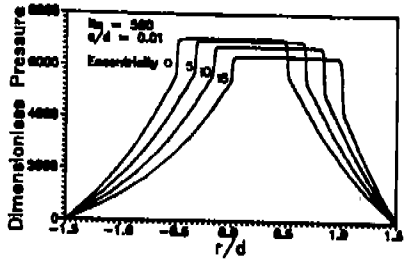

Fig. 7 - Dimensionless pressure distribution for Re=500, s/d=0.01

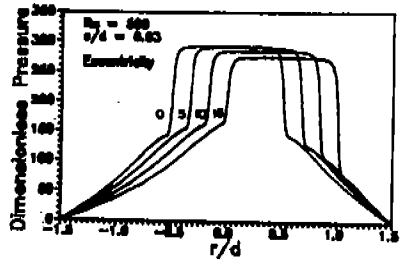

Fig. 8 - Dimensionless pressure distribution for Re=500, s/d=0.03

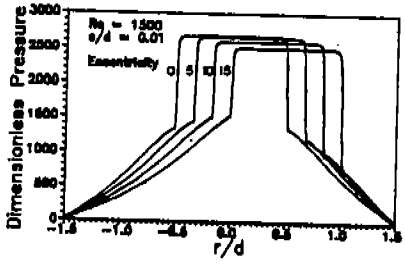

Fig. 9 - Dimensionless pressure distribution for Re=1500, s/d=0.01

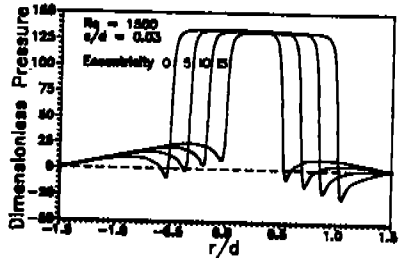

Fig. 10 - Dimensionless pressure distribution for Re=1500, s/d=0.03

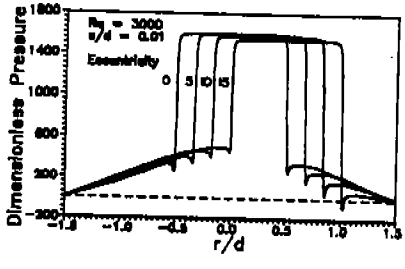

Fig. 11 - Dimensionless pressure distribution for Re=3000, s/d=0.01

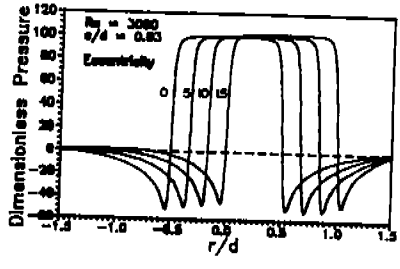

Fig. 12 - Dimensionless pressure distribution for Re=3000, s/d=0.03

The results show the great influence of the separation between disks and of the flow Reynolds numbers on the dimensionless pressure distribution, especially for s/d = 0.01. The influence of the eccentricity is relatively small. For s/d = 0.01 there is a reduction of the pressure in the stagnation region for all Reynolds numbers for all eccentricities being analyzed. This means that there is a reduction in the flow resistance due to the eccentricity. For s/d = 0.03 the same tendency is observed for Re = 500 and Re = 1500 in a smaller scale. Nevertheless for Re = 3000 it is observed an inverse tendency, that is, there is an increase in flow resistance which causes a small elevation of the dimensionless pressure in the stagnation region when the eccentricity is increased. This is due to the presence of bigger separation bubbles at the diffuser inlet, reducing the flow cross section, as shown in Fig. 16.

The integration of the dimensionless pressure distribution over the total reed area furnishes the total force caused by the flow itself. In the present work the resulting dimensionless force on the reed is given by Eq. (7).

$$F = \int_{o}^{2\pi} \int_{\eta_2}^{\eta \to \infty} p^* h^2/d^2 \; d\psi \; d\eta \qquad (7)$$

Fig. 13 presents the variation of the dimensionless force on the reed for different Reynolds numbers, and different gaps between disks when the eccentricity is varied. For both gaps under analysis there is a reasonable reduction in the dimensionless force as the flow Reynolds number increases. The influence of the eccentricity for all Reynolds numbers is very small. For s/d = 0.01 it is observed a reduction in the dimensionless force for all Reynolds numbers when the eccentricity increases. However, for s/d = 0.03 the tendency is diverse. For Re = 500, the dimensionless force is slightly reduced when the eccentricity increases, and for Re = 1500 the inverse is observed. This is due to the fact that the dimensionless pressure in the stagnation region remains almost constant while there is an increase in the local pressure in a larger region in the flow, as shown in Fig. 8. The same trend occurs for Re = 3000 where it is observed a small increase in the dimensionless pressure in the stagnation region.

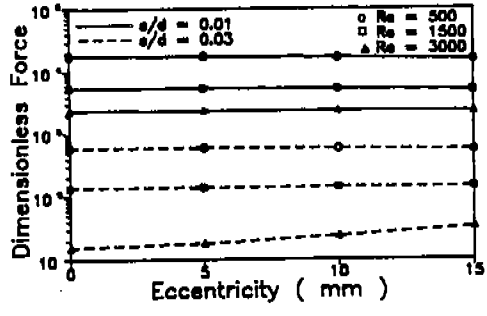

Fig. 13 - Dimensionless force on the reed

An important characteristic of the flow field is the circumferential distribution of the cross section mean velocity at the diffuser outlet Vm, as shown in Fig. 14. V_m is defined as

$$V_m = 1/s \int_{o}^{s} V_\psi \; dz \qquad (8)$$

where V_ψ is the velocity component v in a certain position ψ.

As it can be observed in Fig. 14, there is a non-uniform circumferential distribution of mass flow rate in the eccentric diffuser. This is generated by the variable flow resistance imposed by the solid boundaries. A greater solid overlapping reduces the directional mass flow rate (ψ = 0). This effect is more important for higher eccentricity values.

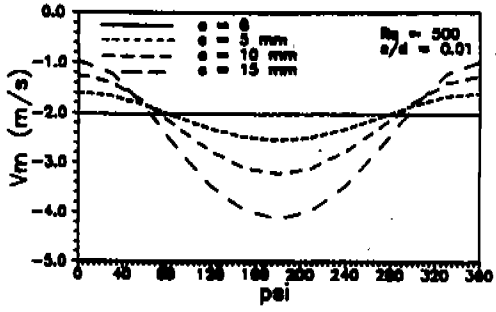

Fig. 14 - Circumferential mean velocity distribution at the diffuser outlet

The reattachment length, ΔS_η is another important parameter to get a better understanding of the flow field in the diffuser region. It defines the recirculating region caused by the effect of flow curvature at the exit of the feeding orifice. Fig. 15 presents the variation of the reattachment length as a function of flow Reynolds number for s/d = 0.01 and 0.03.

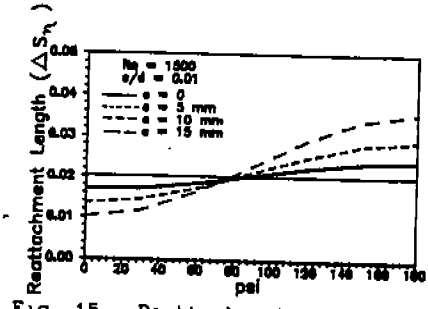

Fig. 15 - Reattachment length variation with ψ for Re = 1500, s/d = 0.01

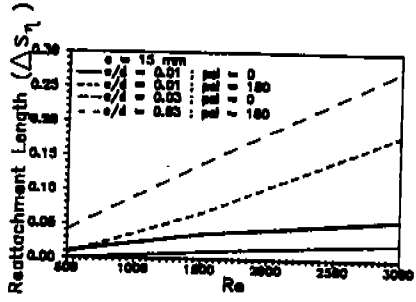

Fig. 16 - Reattachment length variation with Reynolds number

In order to improve the understanding of the pressure flow field over the reed, Figs. 17 and 18 have been prepared.

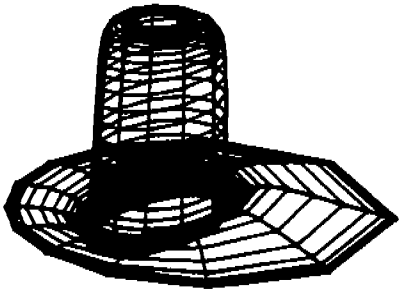

Fig. 17 - Flow pressure field for Re=1500, s/d=0.03, e=10mm

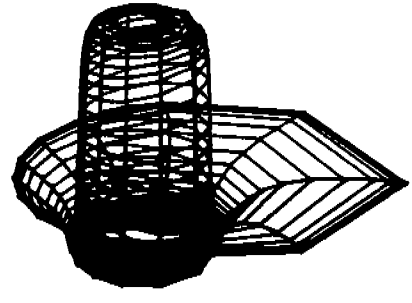

Fig. 18 - Flow pressure field for Re=3000, s/d=0.03, e=15mm

CONCLUSIONS

This paper presents an experimentally validated numerical investigation, using the method of finite volumes, of the laminar, incompressible, isothermal, steady air flow through eccentric radial diffusers. The main motivation for this work is the understanding of fluid flow and thrust in valves of refrigeration compressors.

For a certain eccentricity, it has been observed that there is a great influence of the gap between disks and of the Reynolds number on the dimensionless pressure distribution along the reed, mainly for small gaps. Besides generating a three-dimensional and an asymmetric flow field, modifying considerably the pressure and velocity fields, the eccentricity of the frontal disk does not alter significantly the dimensionless resultant force on the reed, when compared to concentric circular disks. Nevertheless the local loading on the reed used to analyze the distribution of stresses is completely modified when compared to a symmetric valve reed and therefore it should be considered.

BIBLIOGRAPHIC REFERENCES

[01] Deschamps, C.J., Laminar Fluid Flow Through Compressor Valves, M.Sc. Dissertation, Department of Mechanical Engineering, Federal University of Santa Catarina, Brazil, 1987 (in Portuguese).

[02] Ferreira, R.T.S., Deschamps, C.J., Prata, A.T., Pressure Distribution Along Valve Reeds of Hermetic Compressors, Exp. Thermal and Fluid Science, vol. 2, pp. 201-207, 1989.

[03] Patankar, S.V., Numerical Heat Transfer and Fluid Flow. Hemisphere Publ. Corp., Washington, 1980.

[04] Gasche, J.L., Laminar Fluid Flow Through Eccentric Refrigeration Compressor Valves, M.Sc. Dissertation, Department of Mechanical Engineering, Federal University of Santa Catarina, Brazil, 1992 (in Portuguese).

[05] Patankar, S.V., A Numerical Method for Conduction in Composite Materials, Flow in Regular Geometries and Conjugate Heat Transfer, Proc. 6th Intern. Heat Transfer Conf., Vol. 3, pp. 297-304, Toronto, 1978.

[06] Holman, J.P., Experimental Methods for Engineers, McGraw Hill, Tokyo, 1981.